

AD-A 122 198

RIA-82-U478

AD

TECHNICAL REPORT ARLCB-TR-82034

CYCLIC TORSION OF A CIRCULAR
CYLINDER

P.C.T. CHEN
M.R. ABOUTORABI
H.C. WU

TECHNICAL
LIBRARY

DTIC QUALITY INSPECTED 2

OCTOBER 1982



US ARMY ARMAMENT RESEARCH AND DEVELOPMENT COMMAND
LARGE CALIBER WEAPON SYSTEMS LABORATORY
BENET WEAPONS LABORATORY
WATERVLIET N.Y. 12189

APPROVED FOR PUBLIC RELEASE; DISTRIBUTION UNLIMITED

19970930 117

DISCLAIMER

The findings in this report are not to be construed as an official Department of the Army position unless so designated by other authorized documents.

The use of trade name(s) and/or manufacture(s) does not constitute an official indorsement or approval.

DISPOSITION

Destroy this report when it is no longer needed. Do not return it to the originator.

REPORT DOCUMENTATION PAGE		READ INSTRUCTIONS BEFORE COMPLETING FORM
1. REPORT NUMBER ARLCB-TR-82034	2. GOVT ACCESSION NO.	3. RECIPIENT'S CATALOG NUMBER
4. TITLE (and Subtitle) CYCLIC TORSION OF A CIRCULAR CYLINDER		5. TYPE OF REPORT & PERIOD COVERED Final
		6. PERFORMING ORG. REPORT NUMBER
7. AUTHOR(s) P. C. T. Chen M. R. Aboutorabi (University of Iowa) H. C. Wu (University of Iowa)		8. CONTRACT OR GRANT NUMBER(s)
9. PERFORMING ORGANIZATION NAME AND ADDRESS US Army Armament Research & Development Command Benet Weapons Laboratory, DRDAR-LCB-TL Watervliet, NY 12189		10. PROGRAM ELEMENT, PROJECT, TASK AREA & WORK UNIT NUMBERS AMCMS No. 611102H600011 DA Project.1L161102AH60 PRON No 1A2250041A1A
11. CONTROLLING OFFICE NAME AND ADDRESS US Army Armament Research & Development Command Large Caliber Weapon Systems Laboratory Dover, NJ 07801		12. REPORT DATE October 1982
		13. NUMBER OF PAGES 22
14. MONITORING AGENCY NAME & ADDRESS (if different from Controlling Office)		15. SECURITY CLASS. (of this report) UNCLASSIFIED
		15a. DECLASSIFICATION/DOWNGRADING SCHEDULE
16. DISTRIBUTION STATEMENT (of this Report) Approved for public release; distribution unlimited		
17. DISTRIBUTION STATEMENT (of the abstract entered in Block 20, if different from Report)		
18. SUPPLEMENTARY NOTES Presented at US Army Symposium on Solid Mechanics, Red Jacket Beach Motor Inn, So. Yarmouth, Cape Cod, MA, 21-23 September 1982.		
19. KEY WORDS (Continue on reverse side if necessary and identify by block number) Circular Cylinder Torsional Loading Cyclic Loading Plasticity Theory Endochronic Theory <i>Math Anal</i> <i>Num Method</i> <i>Revers Stress</i> <i>Plastic Deformation</i>		
20. ABSTRACT (Continue on reverse side if necessary and identify by block number) The improved endochronic theory of plasticity is applied to the case of a solid bar with circular cross-section subjected to cyclic fully-reversed torsional loading. Numerical techniques are employed to obtain the solution. The parameters of the constitutive equations are determined from the test data of thin-walled specimens. These parameters are then used without alteration of compute stress distributions within the solid specimen. The relation of torque (CONT'D ON REVERSE)		

20. ABSTRACT (CONT'D)

vs. strain at the outermost fiber of the solid specimen provides an ultimate check of this theory. This report demonstrates an expanded use of improved theory.

TABLE OF CONTENTS

	<u>Page</u>
INTRODUCTION	1
BRIEF SUMMARY OF IMPROVED ENDOCHRONIC THEORY	1
DESCRIPTION OF CYCLIC SHEAR RESPONSE	3
TORSION OF A CIRCULAR CYLINDER	5
COMPUTATION	7
RESULTS AND DISCUSSION	8
REFERENCES	11

LIST OF ILLUSTRATIONS

1. Shear Stress-Strain Curves for Thin-Walled Specimens.	12
2. Torque Shear-Strain Curves for Solid Circular Cylinder.	13
3. Stress Distribution at Different Stages of First Loading of Solid Cylinder.	14
4. Stress Distribution at Different Stages of First Unloading of Solid Cylinder.	15
5. Residual Stress Distribution at Zero Torque.	16
6. Theoretical Shear Stress-Strain Behavior of a Hypothetical Material.	17
7. Residual Stress Distribution in a Solid Cylinder (Hypothetical Material).	18

INTRODUCTION

Experimental observations indicate that when metallic materials are subjected to cyclic torsional loading, a hardening behavior similar to the case of uniaxial loading occurs. In a previous paper, Wu and Yip¹ successfully applied the endochronic theory of plasticity to describe the cyclic hardening phenomenon under uniaxial loading, and it is the objective of this report to apply this theory to the case of cyclic torsional loading of a thin-walled cylinder and a solid cylinder of circular cross-section and investigate the residual stress distribution.

BRIEF SUMMARY OF IMPROVED ENDOCHRONIC THEORY

The endochronic theory of plasticity developed by Valanis² is based on the notion of intrinsic time and the internal variable theory of thermodynamics. The original definition of intrinsic time has led to difficulties in cases where the history of deformation involves unloading. Valanis³ has since introduced a new concept on intrinsic time to overcome these difficulties.

The intrinsic time ζ is a measure of irreversibility. A definition of new intrinsic time which is more closely representative of unloading behavior is given as follows:

¹Wu, H. C. and Yip, M. C., "Endochronic Description of Cyclic Hardening Behavior for Metallic Materials," ASME J. of Eng. Materials and Technology, Vol. 103, July 1981, pp. 212-217.

²Valanis, K. C., "A Theory of Viscoplasticity Without a Yield Surface, Part I and Part II, Archives of Mechanics, Vol. 23, 1971, pp. 517-551.

³Valanis, K. C., "Fundamental Consequences of a New Intrinsic Time Measure - Plasticity as a Limit of the Endochronic Theory," Archives of Mechanics, Vol. 32, 1980, pp. 171-191.

$$d\zeta^2 = d\Omega_{ij} d\Omega_{ij} \quad (1)$$

$$d\Omega_{ij} = de_{ij} - k_1 \frac{ds_{ij}}{2\mu_0} \quad (2)$$

where Ω_{ij} is a strain like tensor, e_{ij} and s_{ij} are deviatoric strain and stress tensors respectively, k_1 is a positive constant such that $0 < k_1 < 1$ and μ_0 is shear modulus.

The general constitutive equation for shear response of a material with an elastic hydrostatic response and no coupling between deviatoric and hydrostatic behavior is:

$$s_{ij} = 2 \int_0^z \mu(z-z') \frac{de_{ij}}{dz'} dz' \quad (3)$$

where z is an intrinsic time which is related to ζ by the following time scale

$$\frac{d\zeta}{dz} = f(\zeta) \quad (4)$$

It has been shown in Reference 3 that $f(\zeta)$ describes isotropic hardening and is therefore termed the hardening function.

Define

$$\mu(z) = \mu_0 G(z) \quad (5)$$

where $G(0) = 1$ indicates initially elastic response. Using Laplace transform technique, (for details see Reference 3), Eq. (3) becomes

$$s_{ij} = 2\mu_0 \int_0^z \rho(z-z') \frac{d\Omega_{ij}}{dz'} dz' \quad (6)$$

³Valanis, K. G., "Fundamental Consequences of a New Intrinsic Time Measure - Plasticity as a Limit of the Endochronic Theory," Archives of Mechanics, Vol. 32, 1980, pp. 171-191.

in which, for the case of $k_1 = 1$,

$$\rho(z) = \rho_0 \delta(z) + \rho_1(z) \quad (7)$$

where $\rho_1(z)$ is composed of a finite sum of exponential terms. A general constitutive equation in terms of initial yield stress s_y and plastic strain Ω_{ij} ($k_1 = 1$) can be obtained as

$$s_{ij} = s_y \frac{d\Omega_{ij}}{dz} + 2\mu_0 \int_0^z \rho_1(z-z') \frac{d\Omega_{ij}}{dz'} dz' \quad (8)$$

by substituting Eq. (7) into Eq. (6) and defining $s_y = 2\mu_0\rho_0$. Note that at $z = 0$:

$$s_{ij} = s_y \left. \frac{d\Omega_{ij}}{dz} \right|_{z=0} \quad (9)$$

Also from Eq. (2), the condition $\Omega_{ij} = 0$ gives the relation,

$$s_{ij} = 2\mu_0 e_{ij} \quad (10)$$

Equation (10) merely attests to the fact that while $z = 0$ the deformation process is reversible and therefore the deviatoric stress response is elastic.

DESCRIPTION OF CYCLIC SHEAR RESPONSE

For pure shear deformation with $\rho_1(z)$ represented by one exponential term, one has

$$d\Omega = d\eta - \frac{d\tau}{2\mu_0} \quad (11a)$$

and

$$2\mu_0 \rho_1(z) = 2\mu_1 e^{-\alpha z} \quad (11b)$$

where η is total shear strain and Ω is plastic shear strain. Eq. (8) yields

$$\tau = \tau_y \frac{d\Omega}{dz} + 2\mu_1 \int_0^z e^{-\alpha(z-z')} \frac{d\Omega}{dz'} dz' \quad (12)$$

with

$$\frac{d\zeta}{dz} = f(z) \text{ and } d\zeta = |d\Omega| \quad (13)$$

and τ_y is the shear yield stress. Using Eqs. (12) and (13) and a suitable function f , the governing equations of torsional test of a thin-walled tube during loading, unloading, and reloading can be derived. The initially elastic unloading (reloading) response and followed Bauschinger effect will be governed by the material property itself, provided that the intrinsic time measure is correct.

If the first unloading of stress-strain curve begins when intrinsic time measure ζ reaches ζ^* , the positive property of ζ requires Eq. (13) to be

$$d\zeta = -d\Omega \quad (14)$$

Define ζ_-^* and ζ_+^* as loading and unloading measures around the neighborhood of ζ^* in ζ space. Then Eq. (12) leads to

$$\tau^- = \tau_y \left. \frac{d\zeta}{dz} \right|_{\zeta_-^*} + 2\mu_1 \int_0^{\zeta_-^*} e^{-\alpha(z-z')} \frac{d\Omega}{dz'} dz' \quad (15)$$

$$\tau^+ = -\tau_y \left. \frac{d\zeta}{dz} \right|_{\zeta_+^*} + 2\mu_1 \int_0^{\zeta_+^*} e^{-\alpha(z-z')} \frac{d\Omega}{dz'} dz' \quad (16)$$

where τ^- and τ^+ are stress states nearby ζ^* at loading and unloading processes respectively. In the limit, when $\zeta_-^* \rightarrow \zeta^*$ and $\zeta_+^* \rightarrow \zeta^*$,

$$\tau^- - \tau^+ = 2\tau_y \left. \frac{d\zeta}{dz} \right|_{\zeta^*} \quad (17)$$

Therefore the shear stress is discontinuous with a discontinuity of magnitude

$$\Delta\tau = 2\tau_y \left. \frac{d\zeta}{dz} \right|_{\zeta^*} \quad (18)$$

in the initially elastic unloading region. If the consequent loading reversals take place at ζ^{**} , ζ^{***} , ... then there is an elastic change of magnitude

$$\Delta\tau = 2\tau_y \left. \frac{d\zeta}{dz} \right|_{\zeta^{**}, \zeta^{***}, \dots} \quad (19)$$

in the shear stress. During these elastic responses the values of ζ and z remain unchanged.

During the elastic response, $d\zeta$ is zero and the constitutive equation is simply

$$d\tau = 2\mu_0 d\eta \quad (20)$$

Once the change is larger than $\tau^- - \tau^+$, then the material behavior is governed by Eq. (12).

TORSION OF A CIRCULAR CYLINDER

In laboratory experiments on torsion of solid bars, the recorded data are usually the strain at the outer fiber and the amount of externally applied torque. In order to describe these experimental results, the shear constitutive equation established in the previous section and based on a thin-walled tubular specimen should be applied together with the equations discussed in this section.

The external torque for a solid bar with a circular cross-section is given as:

$$T_s = 2\pi \int_0^a r \tau^2 dr \quad (21)$$

where τ is current shear stress state corresponding to location r , and r_a is the radius of cross-section. The torque can be approximated by discretizing the circular cross-section into a finite number of concentric circular rings and assuming τ to be constant over each ring. Thus

$$T_s = 2\pi \sum_{i=1}^n \tau_i r_i^2 \Delta r_i \quad (22)$$

Now Eqs. (12) and (13) along with Eq. (11a) can be solved to yield τ_i at each fiber, if the value of η_i (shear strain) at that fiber is known. Geometrical considerations show that radial lines have to remain straight after deformation. Thus, one concludes that

$$\eta_i = \frac{r_i}{r_a} \eta_a \quad (23)$$

where η_a is the strain at the outer-most fiber.

Recall that there is a yield stress introduced in Eq. (8) when $k_1 = 1$ and $\zeta = 0$. Hence, an elastic core always exists during deformation whose radius r_e is easily computed as

$$r_e = \frac{\tau_y}{2\mu_0} \frac{r_a}{\eta_a} \quad (24)$$

If the experiment is strain controlled with strain at r_a varying between $-\eta_a$ and $+\eta_a$, and with η_a in the plastic range, then the elastic core radius remains fixed during all stages of loading after the first load reversal.

Now that η_i is known, the value of shear stress at each fiber can be evaluated and used in Eq. (22). Note that at the points of load reversal, for the fibers in the plastically deformed region, there exists an elastic range governed by Eq. (19). This discrete type formulation of torque has the

advantage of being capable of describing the transient and residual stresses in the bar as well.

COMPUTATION

The governing equations are Eqs. (11a), (12), (13), (22), and (23) which are summarized below:

$$d\Omega = d\eta - \frac{d\tau}{2\mu_0} \quad (11a)$$

$$\tau = \tau_y \frac{d\Omega}{dz} + 2\mu_1 \int_0^z e^{-\alpha(z-z')} \frac{d\Omega}{dz'} dz' \quad (12)$$

$$\frac{d\zeta}{dz} = f(z) \quad \text{and} \quad d\zeta = |d\Omega| \quad (13)$$

$$T_S = 2\pi \sum_{i=1}^n \tau_i r_i^2 \Delta r_i \quad (22)$$

$$\eta_i = \frac{r_i}{r_a} \eta_a \quad (23)$$

Since the analytical solution of these equations is quite involved, and in particular requires different treatment and derivation for different hardening functions $f(z)$, a numerical scheme has been developed to solve the above equations. Since the relationship between ζ , the independent variable, and η , the controlled variable is indirect, iterative techniques are an integral part of this program.

In order to ascertain the degree of accuracy of numerical methods, a hypothetical case was assumed. Namely, the field equations were solved analytically using $f(z) = \exp(\beta z)$, and the results were compared with those

obtained numerically. The difference between the two is so small that using numerical techniques does not introduce any significant amount of error.

RESULTS AND DISCUSSION

Once the accuracy of the computer program was established, it was used to predict the results of experiments performed on annealed AISI 4142 steel. The experimental results of cyclic torsion test obtained by the Plasticity Research Laboratory at the University of Iowa are presented along with the theoretical predictions in Figures 1 and 2. This material does not show any appreciable amount of cyclic hardening.

The most important factor in theoretical predictions is the choice of the hardening function $f(z)$. In this computation, the form

$$\frac{d\zeta}{dz} = C - (C-1)e^{-\beta z} \quad (25)$$

has been used because of its simplicity and its proven usefulness in cases of cyclic loading.

Following accepted procedures, the shear stress-strain curve for the material was obtained from a thin-walled tubular specimen, and the value of the material constant were determined from this data. The values of the constants are: $\alpha = 1100$, $\beta = 30,000$, $C = 1.9$, $\mu_0 = 10^7$ psi (68.9×10^3 MPa), $\mu_1 = 3.6 \times 10^6$ psi (24.8×10^3 MPa), $\tau_y = 6,500$ psi (44.79 MPa). As can be seen from Figure 1 this set of constants predict the experimental results reasonably well. The same set of constants were then used to predict the results for a solid bar test. As evidenced in Figure 2, theoretical and experimental results are in reasonable agreement.

As a consequence of the computational process the distribution of stress in the cross-section is evaluated. Such distribution at different magnitudes of torque during the first loading half-cycle is presented in Figure 3. Notice that the outer fiber is the first one to yield; subsequently as more torque is applied, the radius of the elastic inner core gets smaller. Also note that the rate of hardening for each fiber decreases which is, of course, in accordance with strain hardening phenomenon.

Figure 4 presents the distribution of the shear stress in the bar at different stages of the first unloading. The flat portion in the lower curves corresponds to the fibers which have surpassed this initial elastic unloading and started plastic unloading. An interesting observation can be made here, when the amount of reversed torque gets larger, the size of the plastically deformed region, i.e., the flat portion, gets bigger as well, but for each individual fiber the developed plastic stress does not increase accordingly. Rather, the applied torque is preferably compensated for by elastic relief of shear stress in the internal fibers. In other words, whenever possible the material prefers to behave elastically rather than plastically. This is, of course, natural because energy dissipation associated with elastic behavior is much smaller than that of a plastic one.

The distribution of residual stresses at the end of first cycle where the applied torque is equal to zero, is presented in Figure 5.

For purposes of investigating the implications of the model developed here, a hypothetical material with appreciable cyclic hardening behavior was studied. The shear stress-strain behavior of such material under fully-reversed torsional loading is presented in Figure 6. The material constants

for this material were determined as: $\alpha = 1000$, $\beta = 50$, $C = 1.5$, $\mu_0 = 10^7$ psi (68.9×10^3 MPa), $\mu_1 = 4 \times 10^6$ psi (27.56×10^3 MPa) and $\tau_y = 10,000$ psi (68.9 MPa). A steady loop is established after a few cycles.

Figure 7 presents the residual stress distribution at the end of reversal cycles up to and including the steady loop.

REFERENCES

1. Wu, H. C. and Yip, M. C., "Endochronic Description of Cyclic Hardening Behavior for Metallic Materials," ASME J. of Eng. Materials and Technology, Vol. 103, July 1981, pp. 212-217.
2. Valanis, K. C., "A Theory of Viscoplasticity Without a Yield Surface, Part I and Part II," Archives of Mechanics, Vol. 23, 1971, pp. 517-551.
3. Valanis, K. C., "Fundamental Consequences of a New Intrinsic Time Measure-Plasticity as a Limit of the Endochronic Theory," Archives of Mechanics, Vol. 32, 1980, pp. 171-191.

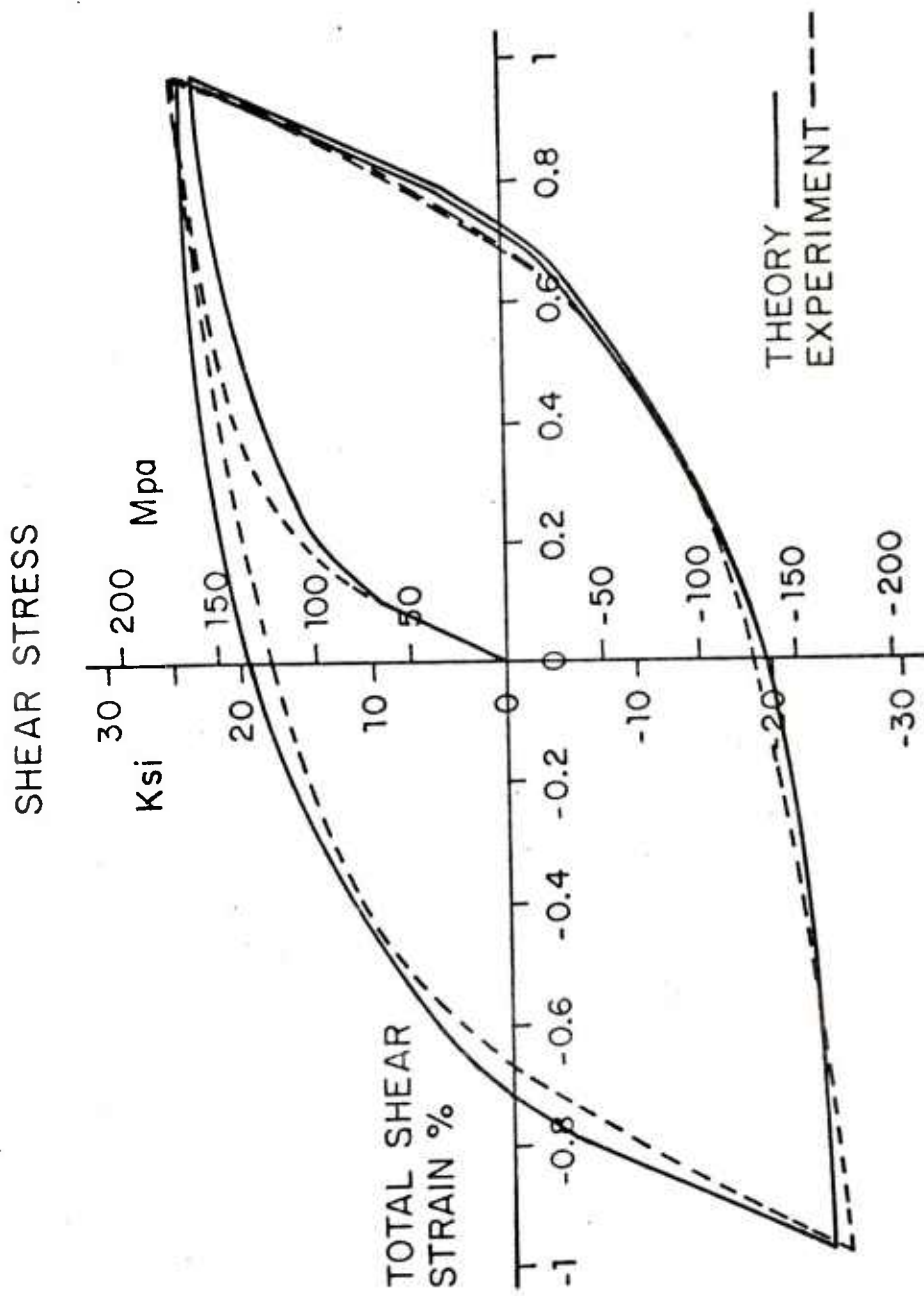


Figure 1. Shear Stress-Strain Curves for Thin-Walled Specimens.

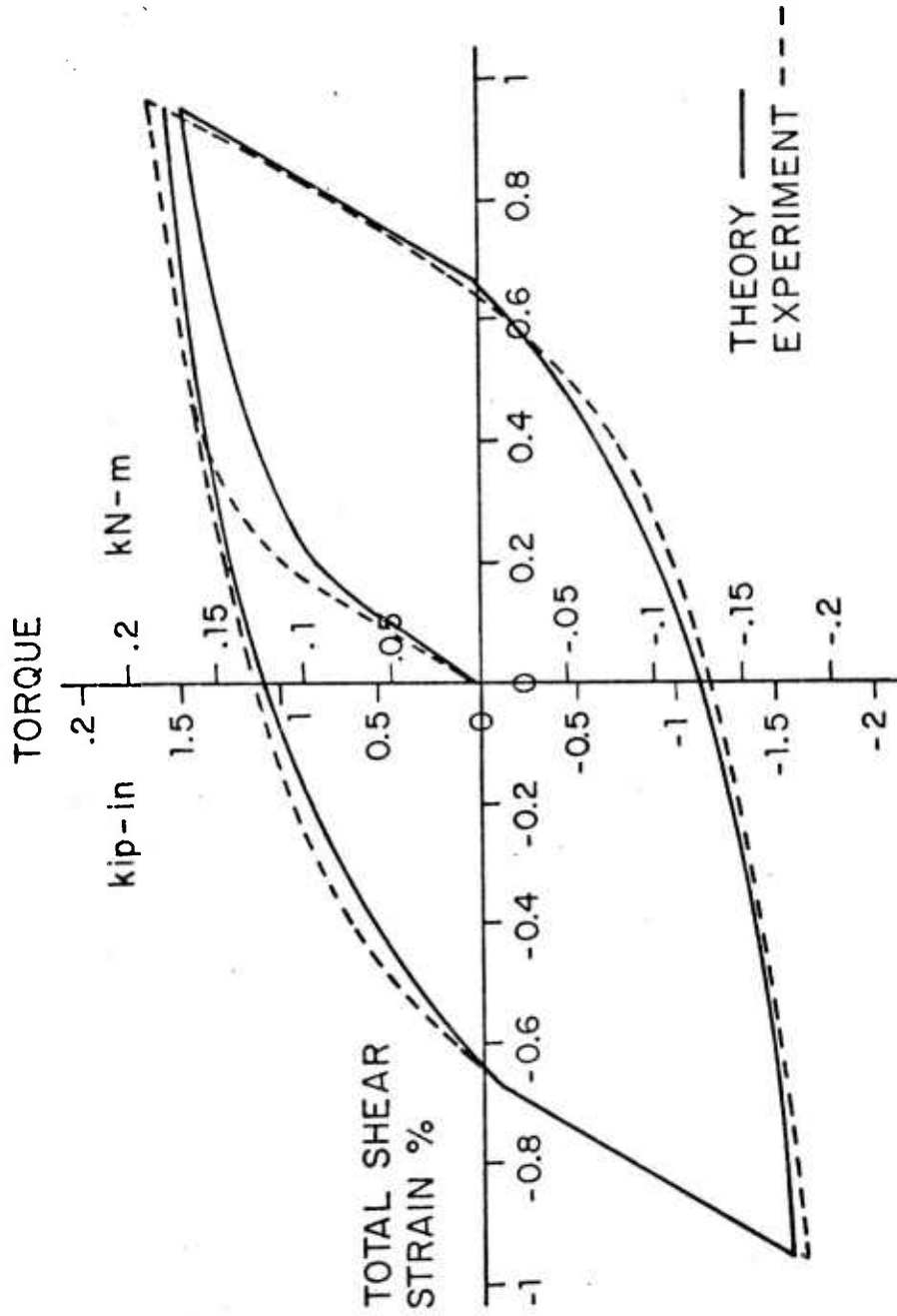


Figure 2. Torque Shear-Strain Curves for Solid Circular Cylinder.

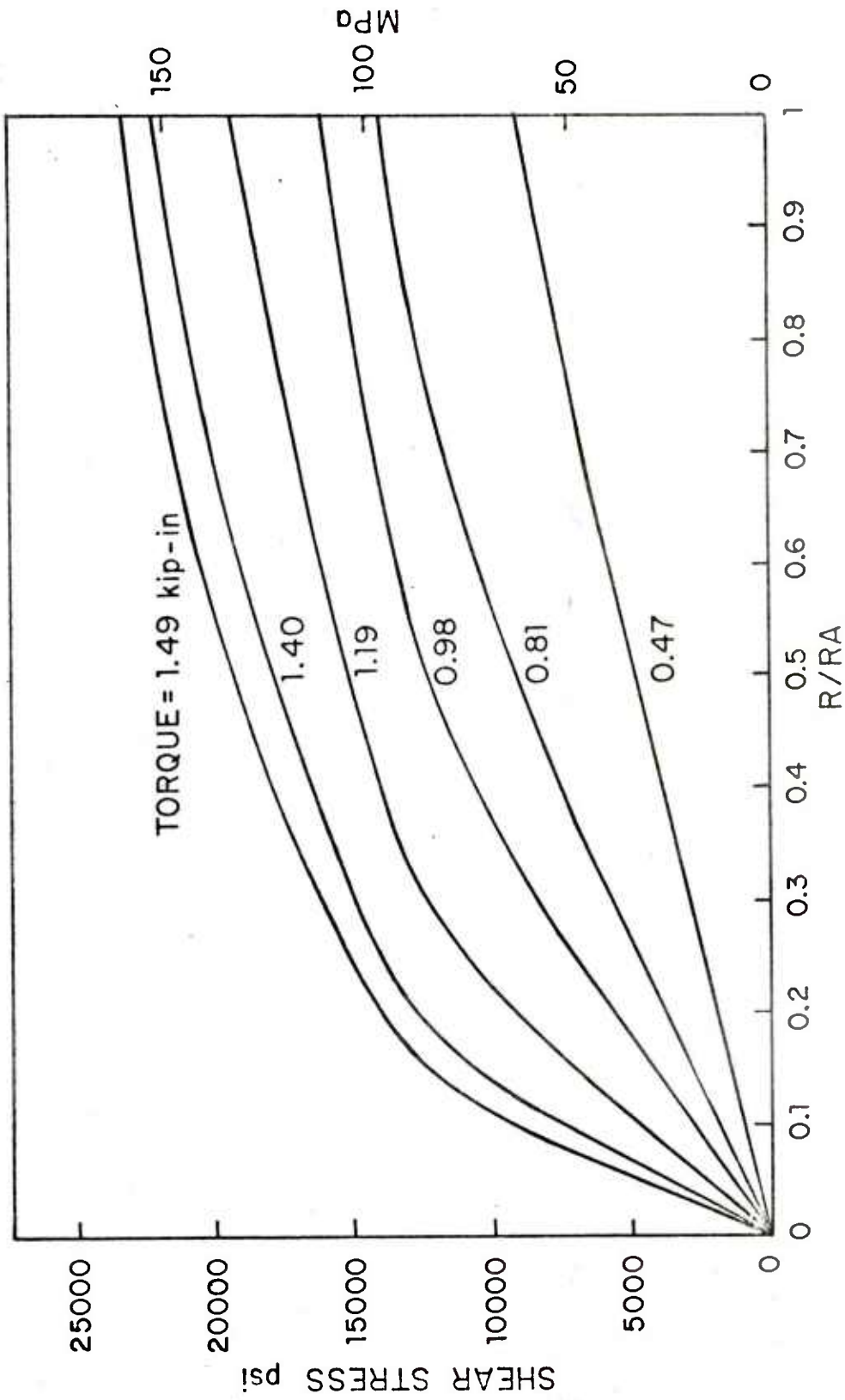


Figure 3. Stress Distribution at Different Stages of First Loading of Solid Cylinder.

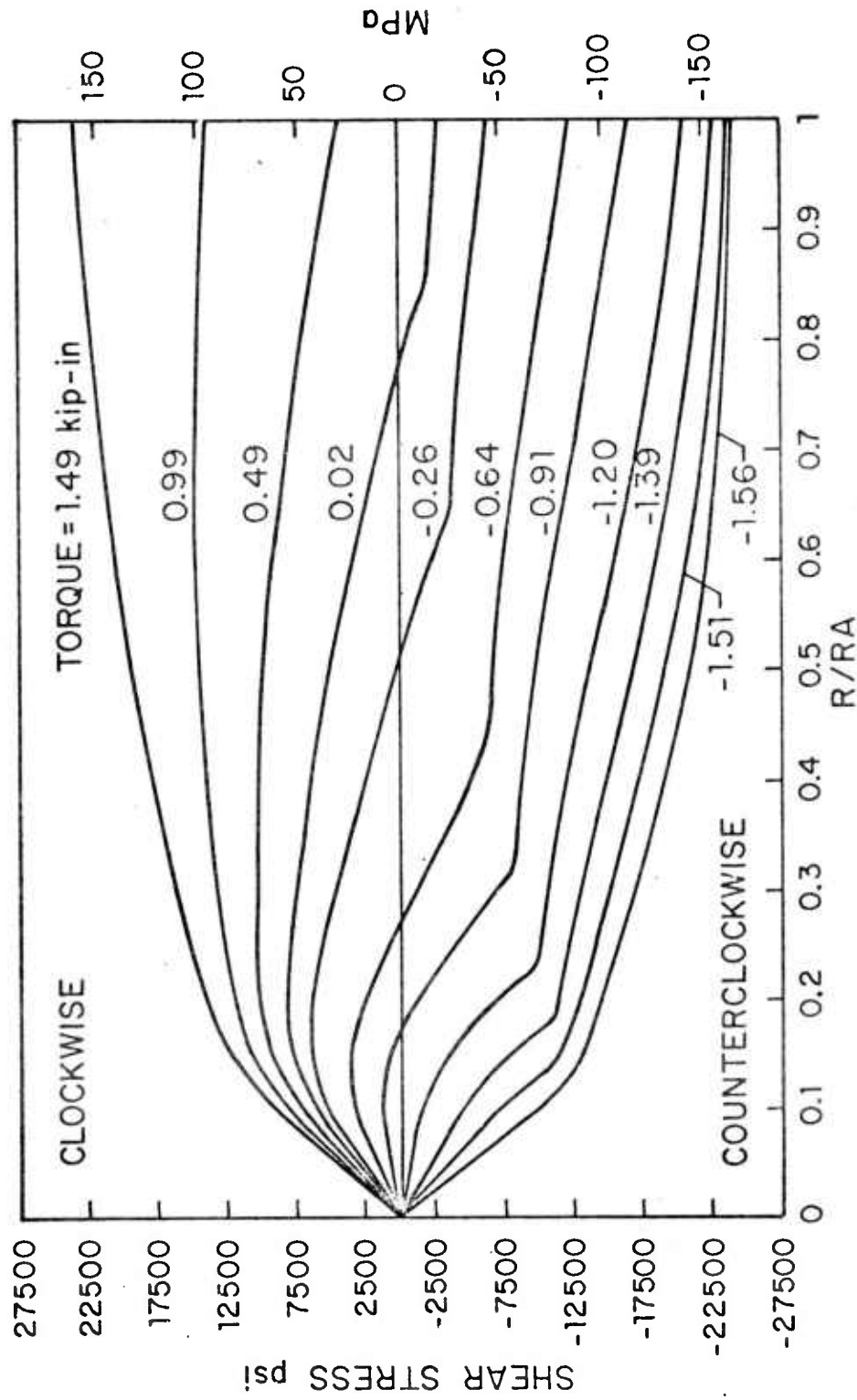


Figure 4. Stress Distribution at Different Stages of First Unloading of Solid Cylinder.

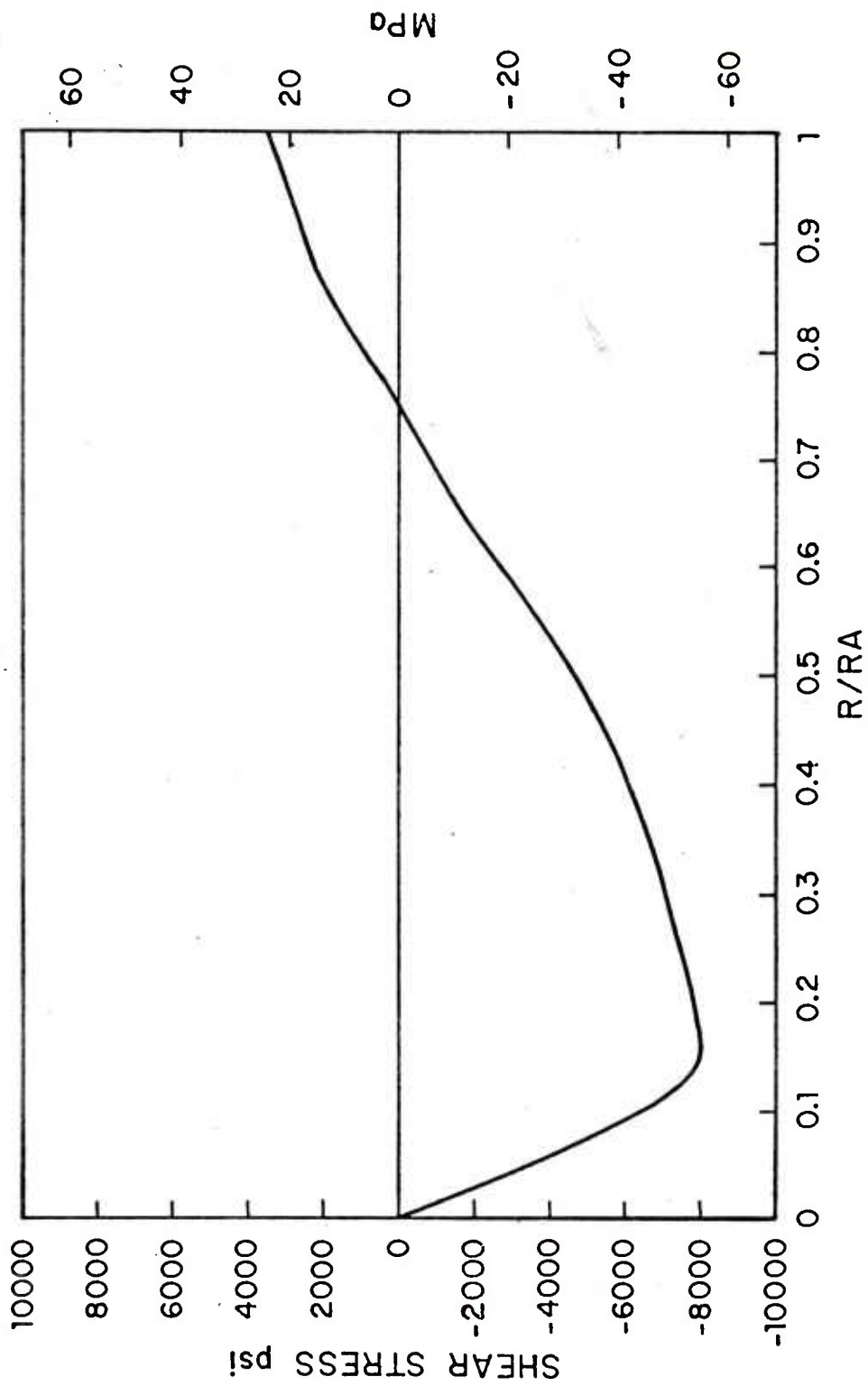


Figure 5. Residual Stress Distribution at Zero Torque.

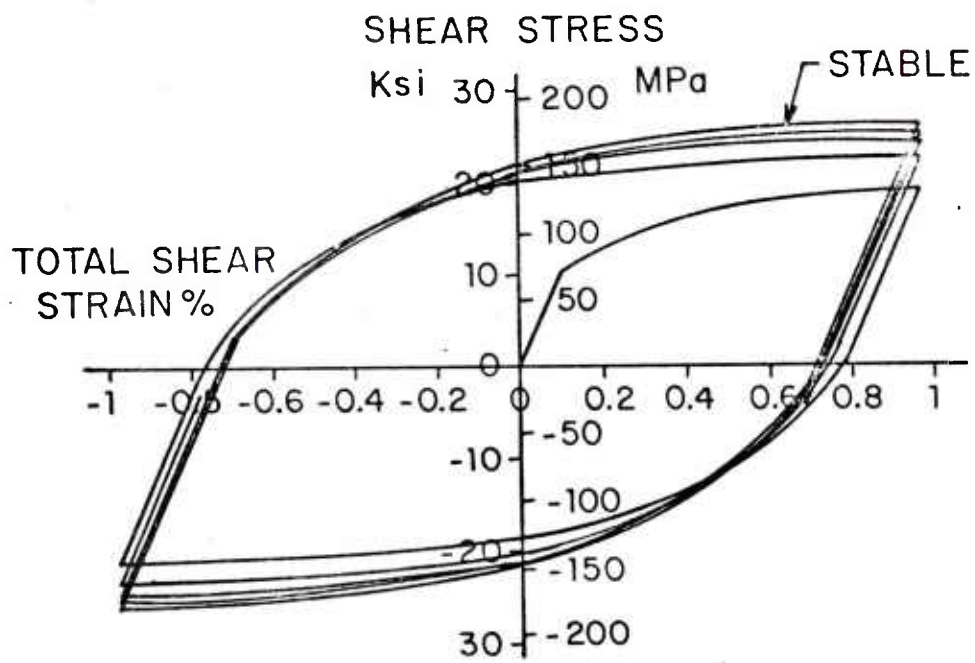


Figure 6. Theoretical Shear Stress-Strain of a Hypothetical Material.

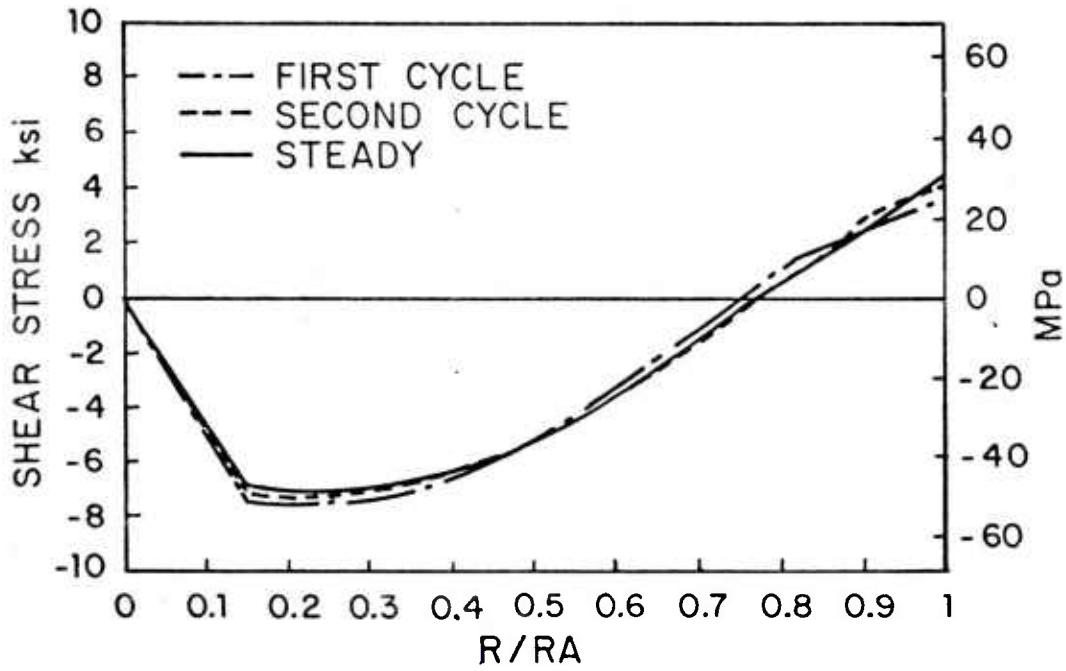


Figure 7. Residual Stress Distribution in a Solid Cylinder (Hypothetical Material).

TECHNICAL REPORT INTERNAL DISTRIBUTION LIST

	<u>NO. OF COPIES</u>
CHIEF, DEVELOPMENT ENGINEERING BRANCH	
ATTN: DRDAR-LCB-D	1
-DP	1
-DR	1
-DS (SYSTEMS)	1
-DS (ICAS GROUP)	1
-DC	1
CHIEF, ENGINEERING SUPPORT BRANCH	
ATTN: DRDAR-LCB-S	1
-SE	1
CHIEF, RESEARCH BRANCH	
ATTN: DRDAR-LCB-R	2
-R (ELLEN FOGARTY)	1
-RA	1
-RM	1
-RP	1
-RT	1
TECHNICAL LIBRARY	5
ATTN: DRDAR-LCB-TL	
TECHNICAL PUBLICATIONS & EDITING UNIT	2
ATTN: DRDAR-LCB-TL	
DIRECTOR, OPERATIONS DIRECTORATE	1
DIRECTOR, PROCUREMENT DIRECTORATE	1
DIRECTOR, PRODUCT ASSURANCE DIRECTORATE	1

NOTE: PLEASE NOTIFY DIRECTOR, BENET WEAPONS LABORATORY, ATTN: DRDAR-LCB-TL,
OF ANY REQUIRED CHANGES.

TECHNICAL REPORT EXTERNAL DISTRIBUTION LIST

	<u>NO. OF COPIES</u>		<u>NO. OF COPIES</u>
ASST SEC OF THE ARMY RESEARCH & DEVELOPMENT ATTN: DEP FOR SCI & TECH THE PENTAGON WASHINGTON, D.C. 20315	1	COMMANDER ROCK ISLAND ARSENAL ATTN: SARRI-ENM (MAT SCI DIV) ROCK ISLAND, IL 61299	1
COMMANDER DEFENSE TECHNICAL INFO CENTER ATTN: DTIC-DDA CAMERON STATION ALEXANDRIA, VA 22314	12	DIRECTOR US ARMY INDUSTRIAL BASE ENG ACT ATTN: DRXIB-M ROCK ISLAND, IL 61299	1
COMMANDER US ARMY MAT DEV & READ COMD ATTN: DRCDE-SC 5001 EISENHOWER AVE ALEXANDRIA, VA 22333	1	COMMANDER US ARMY TANK-AUTMV R&D COMD ATTN: TECH LIB - DRSTA-TSL WARREN, MI 48090	1
COMMANDER US ARMY ARRADCOM ATTN: DRDAR-LC DRDAR-LCA (PLASTICS TECH EVAL CEN)	1	COMMANDER US ARMY TANK-AUTMV COMD ATTN: DRSTA-RC WARREN, MI 48090	1
DRDAR-LCE	1	COMMANDER US MILITARY ACADEMY ATTN: CHM, MECH ENGR DEPT WEST POINT, NY 10996	1
DRDAR-LCM (BLDG 321)	1		
DRDAR-LCS	1	US ARMY MISSILE COMD	
DRDAR-LCU	1	REDSTONE SCIENTIFIC INFO CEN	
DRDAR-LCW	1	ATTN: DOCUMENTS SECT, BLDG 4484	2
DRDAR-TSS (STINFO)	2	REDSTONE ARSENAL, AL 35898	
DOVER, NJ 07801			
DIRECTOR US ARMY BALLISTIC RESEARCH LABORATORY ATTN: DRDAR-TSB-S (STINFO) ABERDEEN PROVING GROUND, MD 21005	1	COMMANDER US ARMY FGN SCIENCE & TECH CEN ATTN: DRXST-SD 220 7TH STREET, N.E. CHARLOTTESVILLE, VA 22901	1
COMMANDER US ARMY ARRCOM ATTN: DRSAR-LEP-L ROCK ISLAND ARSENAL ROCK ISLAND, IL 61299	1	COMMANDER US ARMY MATERIALS & MECHANICS RESEARCH CENTER ATTN: TECH LIB - DRXMR-PL WATERTOWN, MA 02172	2

NOTE: PLEASE NOTIFY COMMANDER, ARRADCOM, ATTN: BENET WEAPONS LABORATORY, DRDAR-LCB-TL, WATERVLIET ARSENAL, WATERVLIET, NY 12189, OF ANY REQUIRED CHANGES.

TECHNICAL REPORT EXTERNAL DISTRIBUTION LIST (CONT'D)

	<u>NO. OF COPIES</u>		<u>NO. OF COPIES</u>
COMMANDER US ARMY RESEARCH OFFICE ATTN: CHIEF, IPO P.O. BOX 12211 RESEARCH TRIANGLE PARK, NC 27709	1	DIRECTOR US NAVAL RESEARCH LAB ATTN: DIR, MECH DIV CODE 26-27 (DOC LIB) WASHINGTON, D.C. 20375	1 1
COMMANDER US ARMY HARRY DIAMOND LAB ATTN: TECH LIB 2800 POWDER MILL ROAD ADELPHIA, MD 20783	1	METALS & CERAMICS INFO CEN BATTELLE COLUMBUS LAB 505 KING AVE COLUMBUS, OH 43201	1
COMMANDER NAVAL SURFACE WEAPONS CEN ATTN: TECHNICAL LIBRARY CODE X212 DAHLGREN, VA 22448	1	MATERIEL SYSTEMS ANALYSIS ACTV ATTN: DRXSY-MP ABERDEEN PROVING GROUND MARYLAND 21005	1

NOTE: PLEASE NOTIFY COMMANDER, ARRADCOM, ATTN: BENET WEAPONS LABORATORY,
DRDAR-LCB-TL, WATERVLIET ARSENAL, WATERVLIET, NY 12189, OF ANY
REQUIRED CHANGES.